Numerical and experimental testing of aircraft tyre impact during landing

Y. Gan[ID] **and X. Fang**
College of Aerospace Engineering
Nanjing University of Aeronautics and Astronautics
Nanjing
Jiangsu, 210016
China

X. Wei and H. Nie
wei_xiaohui@nuaa.edu.cn
College of Aerospace Engineering
Nanjing University of Aeronautics and Astronautics
Nanjing
Jiangsu, 210016
China
and
State Key Laboratory of Mechanics and Control of Mechanical Structures
Nanjing
Jiangsu, 210016
China

ABSTRACT

The capability of aircraft tyres to sustain landing impact loads is essential for flight landing safety. Hence, the development of a reliable experimental database is necessary to validate numerical models. The experimental data on aircraft tyre landing impact in the public literature are somewhat sparse. This paper describes a detailed design rig for aircraft tyre impact testing. A finite element model is then created and simulated using a finite element tool (ABAQUS). Inflation and static load simulations are analysed based on the FE tyre model to confirm its reliability. Comparison of experimental measurements with the results reveals that the model can predict the significant features of aircraft tyre impact in a landing scenario. Very little experimental data are publicly available to verify aircraft tyre models. Therefore, the experimental data in this paper fill this gap in the literature.

NOMENCLATURE

$U,$	strain energy density
$\bar{J}_{e1},$	elastic volume ratio
$\bar{I}_1,$	first invariant of deviatoric strain
$C_{i0},$	shear behaviour
$D_i,$	compressibility
$\ddot{x}_n,$	acceleration vectors
$\dot{x}_n,$	velocity vectors
$F_n^{\text{int}},$	vector of internal forces
$F_n^{ext},$	vector of external forces
$\omega_{\max},$	highest element frequency in the mesh

1.0 INTRODUCTION

Aircraft tyres play a crucial role in supporting heavy loads, including passengers, luggage and the aircraft's entire weight. The primary purpose of an aircraft tyre is to provide mobility for the aircraft when on the ground, but they also assist the shock strut in reducing the impact of landing and absorb much of the roughness during take-off as well as providing traction for stopping. In this sense, tyre design against failure caused by impact loads that arise in landing situations is of fundamental importance. Many safety studies have been performed on automobile tyres, but few on aircraft tyres[1].

This paper follows findings from previous research. Kilner[2] developed a tyre model to predict the vertical and drag loads in response to sizeable discrete surface obstacles shorter than the tyre footprint length. Anson et al.[3] described the specific conditions under which Michelin applies Finite Element Analysis (FEA) to radial aircraft tyres, included the model definition, calculated tyre displacement and rim contact pressure distributions. Bolarinwa and Olatunbosun[4] described a brief study on the complexity of aircraft tyre structure, the main goal being to investigate how Finite Element (FE) models of the tyre can capture complex behaviour related to the accurate prediction of real tyre behaviour. Reid et al.[5] performed a laboratory test to develop a new tyre model that considers the major components of a tyre. Guo et al.[6] developed a full-scale LS-Dyna FE model that replicates the actual geometry of the target aircraft test tyre to assess its safety criteria in an impact scenario. Baranowski et al.[7] developed a novel and detailed discrete model for a tyre using simulations with cord arrangements that correspond to the actual tyre. Yao et al.[8] established a detailed finite element model of an aircraft tyre based on the target tyre's actual geometry for dynamic numerical simulations. Essienubong et al.[9] established a three-dimensional finite element model of a tyre using the finite element tool LS-DYNA and investigated the effect of increasing the landing weight on the tyre performance. Zhang et al.[10] coupled smoothed particle hydrodynamics and the finite element method in LS-DYNA to carry out research work on aircraft tyre spray.

Note that few studies or experimental data have been published on aircraft tyres in landing scenarios. This provides the motivation for the present study, which explores the response of aircraft tyres to impact loads. The aircraft tyre was fixed using a specially designed stand used

Table 1
Test conditions adopted in the experimental programme

Variable	Units	Low	Middle	High
Velocity	m/s	1	1.5	2
Impact mass	kg	246.8	295.7	357.2
Inflation pressure	kPa	550	618	680

for testing, and guides were used to drive an impact mass onto the tyres. Tests were carried out using various combinations of inflation pressure, impact mass and vertical velocity. Since the tests were performed with the tyres rigidly fixed to the stand, no shock absorber systems were considered. Although less realistic, this approach represents a better scenario for comparison with the finite element analysis. Section 2 presents the adopted experimental procedures, followed by a description of the finite element model. The inflation and static load simulations are analysed based on the FE tyre model to indicate its reliability in Section 3. Section 4 presents both the numerical and experimental results, as well as a thorough discussion. Section 5 gives a brief conclusion.

2.0 EXPERIMENTAL AND MODELLING DETAILS

The impact tests involved a tyre/rim set rigidly fixed in a designed stand whose construction enables the tyre to move only in the direction of loading. In this test, the sufficient dropping weight consists of a fixture, hanging basket and additional weights. The height of the drop test is adjusted to simulate different vertical velocities.

For a given wheel, up to 18 impact tests were performed. This study considered three variables: the impact mass, the impact velocity and the tyre pressure. The impact mass and tyre pressure were chosen based on the rated values; the impact velocity was chosen based on the aircraft's actual vertical velocity. Three different aircraft weight load cases were assumed and applied to the tyre: standard weight at 295.7kg, under-loaded at 246.8kg and over-loaded at 357.2kg. The vertical velocity during normal landing is between 1 and 2m/s. For the internal pressure, the rated value of 618kPa was used, as recommended by the tyre manufacturer. This value was also reduced and increased by 10% to further explore the tyre behaviour under impact. Each test was carried out twice to confirm repeatability. Table 1 presents the various test conditions used in the experimental program.

2.1 Structure of aircraft tyre test system

The aircraft tyre test system consists of an impact platform system, a low-friction sliding system, the vertical movement system, the fixture system and the acquisition system (Fig. 1). The dimensions of the test system frame are 3000mm × 400mm × 4000mm in volume, being composed of structural steel.

The impact test is started in free fall. In the test, the effective impact weight (consisting of the basket and additional weight) simulates the impact load. The height of the basket is adjusted to vary the simulated vertical velocity. Flat concrete is used to simulate the surface of the pavement. The 660 × 200 test aircraft tyre designed by Guilin Lanyu Aircraft Tyre Development Co., Ltd. was attached to the main landing gear of J-5.

Table 2
Detailed technical parameters of the sensors

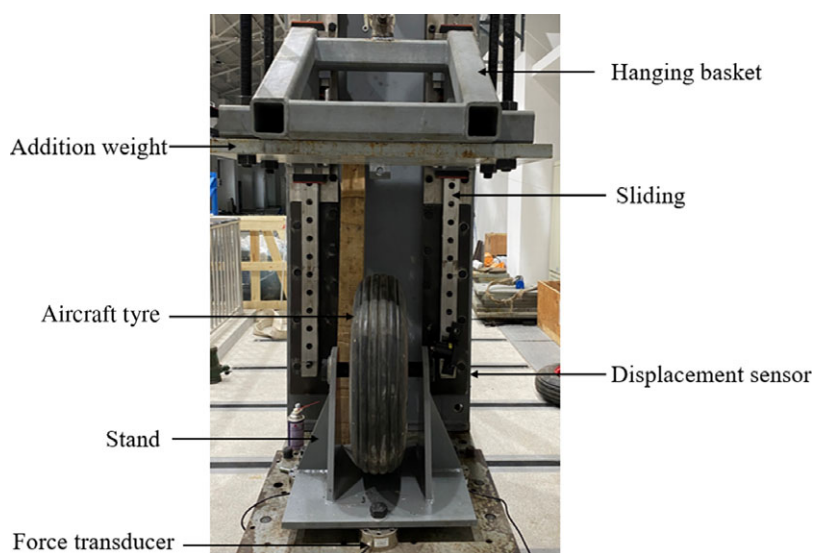| Type	Model	Measurement range	Material	Comprehensive precision
Load sensor 1	JLBU-1	1T	Alloy steel	0.05%F·S
Load sensor 2	JLBU-1	1T	Alloy steel	0.05%F·S
Load sensor 3	JLBU-1	5T	Alloy steel	0.05%F·S
Displacement sensor	5G203	500mm	Hard aluminium	0.3%

Figure 1. Experimental test set-up.

The sliding movement should have certain smoothness to decrease the friction fully, thereby decreasing the errors in the instantaneous vertical velocity of the impact test and ensuring that the test imitates the vertical velocity in the landing process well enough. Three pillars support the impact platform, including vertical sensors.

The parameters that must be measured in the test are as follows: the tyre's vertical impact loads and the vertical displacement of the tyre compression. Three load sensors were installed on the impact platform to measure the vertical load acting on the tyre. A cable displacement sensor is installed between the hanging basket and the sliding system to measure the tyre compression's vertical deflection. The sensors are designed by Jiangsu Donghua Testing Technology Co., Ltd. The detailed technical parameters of the sensors are presented in Table 2.

The whole control system consists of the hydraulic system, the vertical movement mechanism and the telecontrol. Immediately after the electric motor drops the hanging basket to a pre-set height, the hook is locked. As long as the impact system is safely located, the impact system will drop and the test data can be collected.
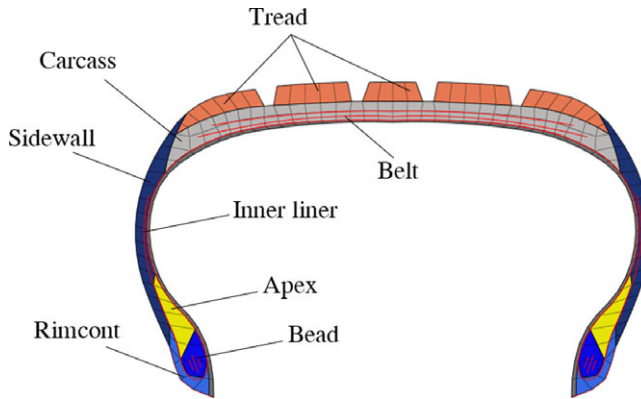
Figure 2. Cross-section of the tyre model.

The data measured in the impact test are collected by the impact test data acquisition system with 24 concurrent channels working at frequencies from 100 to 512kHz (Donghua Testing Technology). A computer was used to log the data and control the impact mass position and its release. A NAC Memrecam HX-7s high-speed camera was used to record the tests at a rate of 2000 frames per second, requiring extra lighting to capture clear pictures.

2.2 Aircraft tyre numerical modelling

A radial (660 × 200) aircraft tyre was used in the finite element model in the present work. The aircraft tyre studied was divided into ten main components in the present Two-Dimensional (2D) section model (Fig. 2). In contrast to the bias tyre, the radial tyre is a kind of pneumatic tyre whose ply cords extend to the beads and are laid substantially at 90° to the centreline of the tread, the carcass being stabilised by an essentially inextensible circumferential belt[11, 12].

The structure and mechanical characteristics of the aircraft tyre are very complex. When building an FE model, the tyre model can be simplified as follows (if the actual requirements permit) to obtain accurate simulation results under the condition of convergence:

1. Only consider longitudinal tread grooves and shallow curbing ribs, and marking lines.
2. This paper mainly analyses the stress of tyre cord and tyre grounding position during the static or dynamic process, simplifies the contact between rim and tyre and sets the tie constraint.
3. Assume that the road is not deformable, as a rigid body.

The 3D tyre model requires rebar layers, making it possible to set different mechanical properties for the various parts of the tyre[13]. The rebar model represents the rebar part (belt) and the matrix part (rubber) by rebar and solid elements. The matrix and rebar elements use the same nodes, and no additional degrees of freedom are introduced. The orientation angle is defined as shown in Fig. 3. Reduced integration and hourglass control were adopted; both sets use default parameter values with scaling factors of 1.

Rubber material usually has long-chain molecules[14]. It exhibits a complicated mechanical behaviour that exceeds the linear elastic theory and includes large deformations, plastic and viscoelastic properties and stress softening[15,16]. The non-linear behaviour of the rubber

Table 3
Rubber properties adopted in the simulation

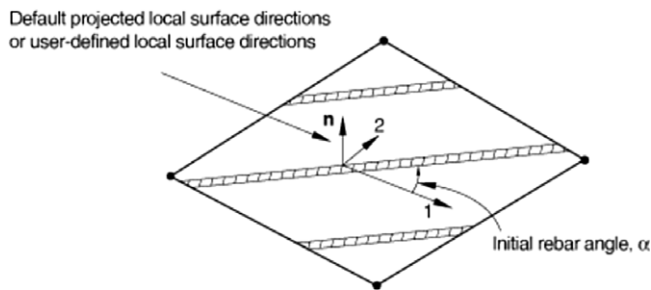| Material	C10	C01	D1	Density (kg/m^3)
Tread	1.0	0	0.0198	1100
Carcass	1.139	0	0.024	1100
Sidewall	1.0	0	0.06	1100
Inner liner	0.953	0	0.03	1100
Apex	1.606	0	0.02	1100
Rimcont	1.406	0	0.02	1100
Bead	0.671	0	0.03	1100

Figure 3. Orientation angle.

part, discretised with 22,800 C3D8R finite elements, is modelled using the Mooney–Rivlin constitutive equation[17,18] whose potential energy of deformation is

$$U = \sum_{i=1}^{N} C_{i0}\left(\bar{I}_1 - 3\right)^i + \sum_{i=1}^{N} \frac{1}{D_i}\left(kern2p\bar{J}_{e1} - 1\right)^{2i} \qquad \ldots (1)$$

where U is the strain energy potential (or strain energy density), that is, the strain per unit of reference volume; $kern2p\bar{J}_{e1}$ is the elastic volume ratio; $\bar{I}_1$ is the first invariant of the deviatoric strain; C_{i0} describes the shear behaviour of the material; D_i introduces compressibility and is set equal to zero for fully incompressible materials; and finally, $N = 1$ is set for the Mooney–Rivlin model. The tyre manufacturer suggests the values for C_{10}, C_{01} and D^1 listed in Table 3, which were adopted in this work.

The bead core was represented by 1200 finite elements (type C3D8R in ABAQUS), adopting the elastic material properties listed in Table 4. The contact between the rim and tyre used tie constraint. The steel cords were modelled as an elastic material using the constants given in Table 4. The reinforcement material properties were considered to be homogeneous and orthotropic. The possible strain-rate sensitivity of the materials was not taken into consideration in the analysis. The belts were defined in the model using surface-type SFM3D4R elements. The reinforcements SURF_BELT-1 and 2 comprise 2600 and 2400 finite elements each. The carcass ply was discretised using 10,800 finite elements. To couple the rubber's reinforcement elements, the restriction embedded element was used for each rebar layer. The geometric properties of the reinforcement materials are presented in Table 5.

Table 4
Reinforcement properties, parameters in the simulation

Material	Young's modulus (N/m^2)	Poisson's ratio	Density (kg/m^3)
Steel belts	8.4×10^{10}	0.4	5900
Bead core	8.4×10^{10}	0.3	5900
Carcass ply	3.3×10^{9}	0.4	5900

Table 5
Geometric properties of reinforcement materials in the simulation

Surface	Cross-sectional (mm^2)	Spacing (mm)	Orientation (degrees)
SURF_BELT-1	0.315	1.22	66
SURF_BELT-2	0.3318	1.27	114
BEAD	0.1869	1.01	90
PLY	0.3848	1.27	0

3.0 FE MODEL VALIDATION IN INFLATION AND STATIC LOAD SCENARIOS

3.1 Inflation scenario

In the inflation scenario, the 2D FE tyre model was mounted to the corresponding wheel rim FE model, being fully constrained at the bearing. The volume of the tyre was inflated to the value of 618kPa recommended by the tyre manufacturer. There are different ways to model the tyre pressure[19–22].

The deformations of the tyre section width and outer diameter were chosen to examine the reliability of the tyre FE model (Fig. 4). The FE model's dimensions at a specific pressure from the simulations were compared with the experimental tyre data in physical tests to validate the accuracy of the FE model.

Table 6 poresents the validation results between the inflation tests and simulation. The simulation results show satisfactory outcomes and close agreement with the test results. The tyre section width shows only a 1.8% difference, whereas the outer diameter exhibits only a 0.7% difference.

3.2 Static load scenario

It is worth mentioning that the aircraft tyre is designed to operate at a specific deflection within its rated load capability, so it is essential to measure the static loaded radius for aircraft safety. The static loaded radius is the perpendicular distance between the axle centreline and a flat surface for a tyre initially inflated to the unloaded rated inflation pressure and then loaded to its rated load[8] (Fig. 5).

Table 6
Tyre inflation test and simulation results

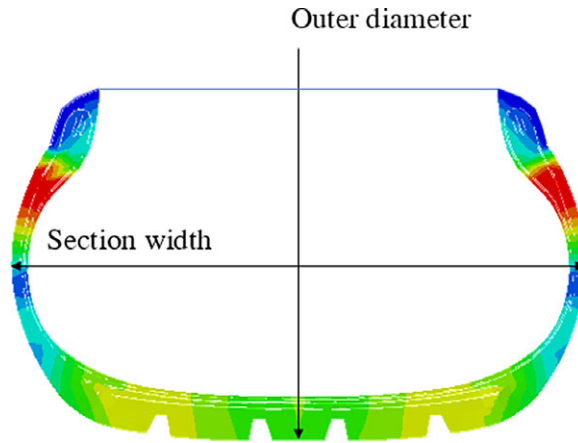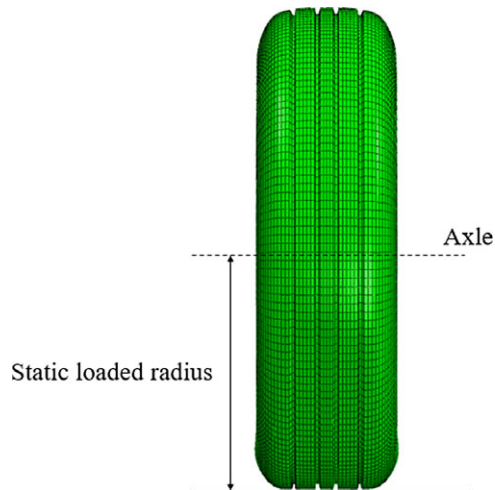|	Section width (mm)	Outer diameter (mm)
Test 1	182.4	650.4
Test 2	182.0	649.8
Average	182.2	650.1
Simulation	185.5	654.4
Difference (%)	1.8	0.7

Figure 4. Tyre cross-section after inflation.

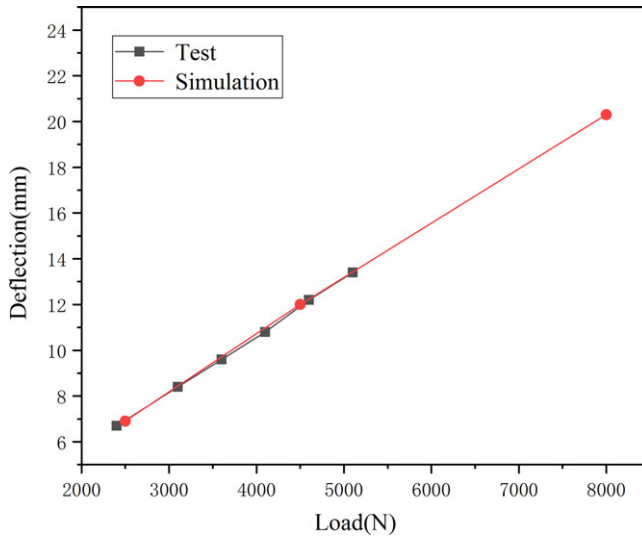Figure 5. Deformation of aircraft tyres in static load scenario.

Figure 6. Deflection versus vertical load curves.

The vertical tyre load versus static deflection curve can be constructed from the different vertical static deflections due to other tyre loading conditions with a fixed tyre inflation pressure of 0.618MPa. The deflections under a fixed tyre inflation pressure of 0.618MPa and different loading conditions from the simulation results are compared with the experimental data.

The tyre inflation pressure is fixed at 0.618MPa, the loads are 8000, 4500 and 2500N and the simulated deflections are 20.3, 12.0 and 6.9mm, respectively. The experimental deflections are 13.4, 12.2, 9.6, 8.4 and 6.7mm for 5100, 4600, 4100, 3600, 3100 and 2400N. These give the vertical load versus static deflection curves in Fig. 6. Again, the simulation results match the experimental measurements very well. The simulation results and experimental measurements agree excellently with previous research[23,24].

4.0 DYNAMIC SIMULATION AND ANALYSIS

During the investigations, the central difference method for integration over time was adopted, which is one variant of the finite difference method. Assuming minimal time steps, the equilibrium equation can be expressed as

$$M\ddot{x}_n + C_d\dot{x}_n + F_n^{\text{int}} = F_n^{ext} \qquad \dots (2)$$

where $\ddot{x}_n$, $\dot{x}_n$ are the acceleration and velocity vectors at t_n, $F_n^{\text{int}} = K_n x_n$ is the vector of internal forces at t_n and F_n^{ext} is the vector of external forces at t_n.

The following solution of the above equation can be obtained by numerical integration of the acceleration $\ddot{x}_n$ under the assumption that $\dot{x}_n \approx \dot{x}_{n-1/2}$:

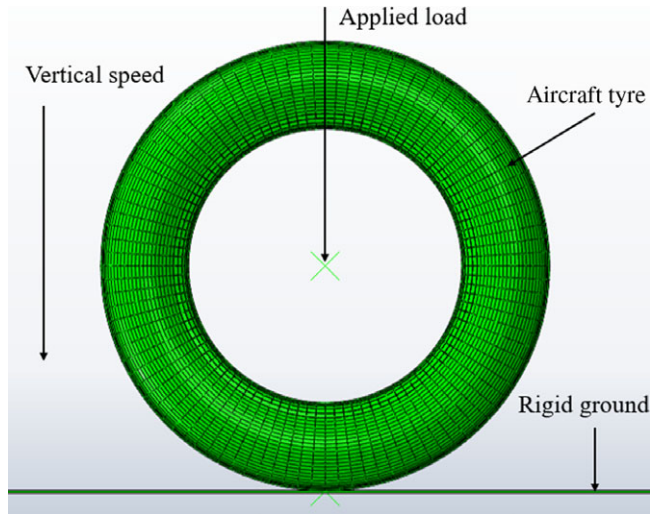$$\ddot{x}_n = M^{-1}\left(p_n - C\dot{x}_{n-1/2} - F_n^{\text{int}}\right) \qquad \dots (3)$$

Figure 7. FE model of aircraft tyre in ABAQUS.

And the implementation of the central difference equations for the velocity and displacement results in

$$\ddot{x}_n = \frac{1}{\Delta t_n}\left(\dot{x}_{n+1/2} - \dot{x}_{n-1/2}\right) \Rightarrow \dot{x}_{n+1/2} = \dot{x}_{n-1/2} + \Delta t_n \ddot{x}_n \qquad \dots (4)$$

$$\dot{x}_{n+1/2} = \frac{1}{\Delta t_{n+1/2}}\left(x_{n+1} - x_n\right) \Rightarrow x_{n+1} = x_n + \Delta t_{n+1/2}\dot{x}_{n+1/2} \qquad \dots (5)$$

The major advantage of this method is the lack of time-consuming operations involving stiffness matrix inversion. Instead, only a diagonal matrix of mass is inverted. However, the main disadvantage is that this method is conditionally stable, implying the following limitation on the time step according to the stability condition:

$$\Delta t \leq \Delta t_{\text{crit}} = \frac{2}{\omega_{\text{max}}} \qquad \dots (6)$$

where ω_{max} is the highest element frequency in the mesh.

Dynamic numerical calculations simulate the whole tyre impact process in ABAQUS (Fig. 7). The non-deformable ground uses a rigid model. The interaction between the tyre and rigid ground is simulated using a contact procedure based on the penalty method with the friction coefficient set to zero. The aircraft weight is included by assigning a concentrated mass at the node at the centre of the tyre, and gravitational loading is also applied to the whole tyre model. Furthermore, the vertical landing speed is included by using a command on the tyre and rim model to predefine the initial velocity field. The initial boundary conditions in the FEA corresponded to the experiments. The simulation was carried out with a 16-core AMD Ryzen 9 3950X supercomputer (each core having two CPUs at 1.6GHz). The whole simulation process took 60min to run.

Table 7
Test and simulation conditions

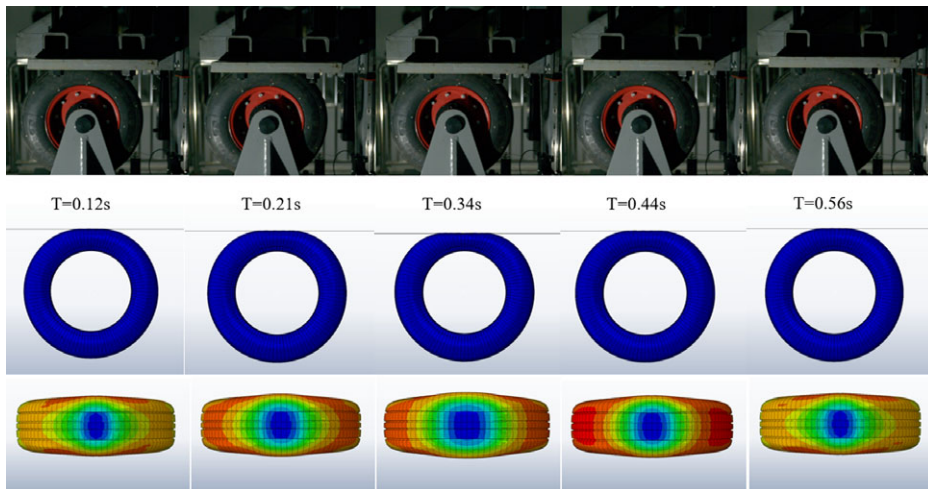| Case	Impact mass (kg)	Inflation pressure (kPa)	Velocity (m/s)
Test	295.7	618	1.5
Simulation	295.7	618	1.5

Figure 8. Comparison of experimental and simulation images.

According to technical documents[25], three parameters are chosen to analyse the maximum impact force:

1. Impact mass. The landing impact mass is important for the safety of aircraft tyres. According to the airworthiness standard, aircraft tyres can be used when the load is beow the rated load.

2. Inflation pressure. The use of an appropriate tyre pressure is important for its performance, and the inflation value is set to prevent the tyre from exceeding the design deflection.

3. Velocity. The variation of the vertical landing velocity is significant for crashworthiness certification and analysis.

5.0 RESULTS

In the dynamic impact scenario, it is evident from Fig. 8 that the simulation also performs well. This figure compares the numerical tyre's deformation profile side by side with images of actual tests captured by the high-speed camera. The impact condition is presented in Table 7.

The recordings from the displacement and force sensors made it possible to obtain the deformation of the hanging basket during its collision with the tyre, as well as the impact
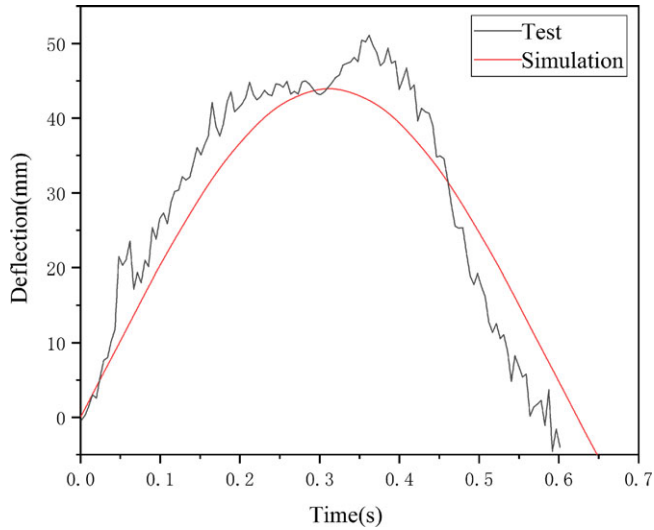
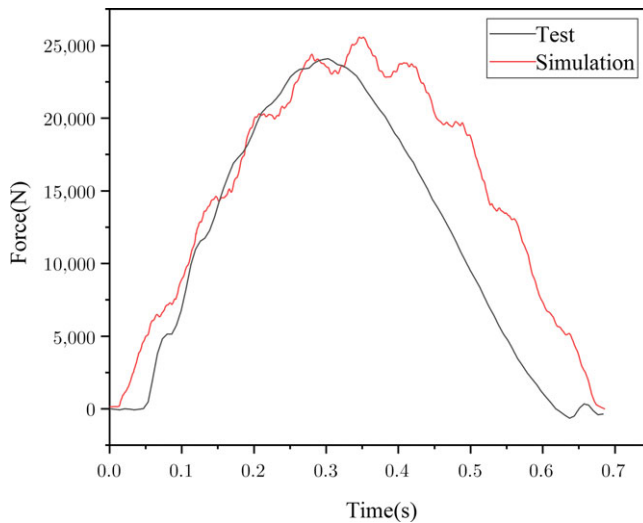Figure 9. Experimental and simulated deflection.

Figure 10. Experimental and simulated force.

load. Figures 8–11 compare the experimental deformation, load and velocity curves for the impact scenario versus the numerical simulation. Figures 9–11 show the results for the impact conditions presented in Table 7.

6.0 DISCUSSION

Overall, the numerical and experimental results presented herein indicate that modelling of a complex structure like an aircraft tyre was successfully achieved. This is especially apparent
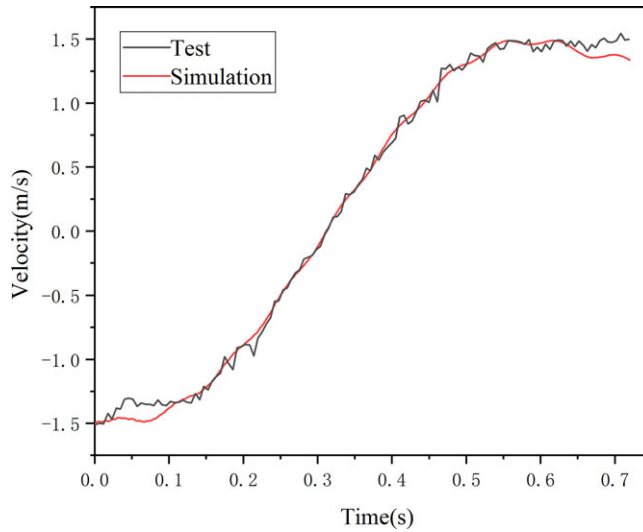
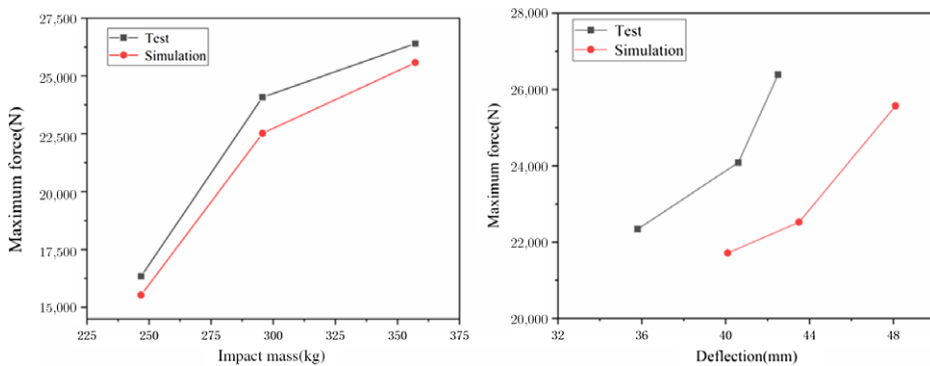Figure 11. Experimental and simulated velocity.

Figure 12. Force versus impact mass and force versus deflection in case A.

from Figs 9–11, which show experimental versus numerical data and indicate both the quality of the simulation and the capability of the experimental setup to capture the significant features of the impact scenario for aircraft tyres.

The time history of tyre deflections is presented in Fig. 9, revealing a monotonic increase to reach a peak value of 43.5mm at 0.34s. After passing this peak, the deflection decreases with time, indicating that the tyre reached its maximum deformation and then began to rebound. This curve describes the basic variation tendency of the deflection in a landing scenario. In the numerical model, the ground was assumed to be non-deformable, thus affecting the tyre behaviour during impact.

Figure 12 shows the variation in the load for increasing impacts. Case A establishes the basic parameters to study the effects of the impact mass and impact force. There was a smaller increase in the maximum force for impact masses greater than versus less than 300kg. When the tyre is compressed to a certain extent, the stiffness changes non-linearly. According to these results, the difference between the experimental and numerical values is 6.5%.
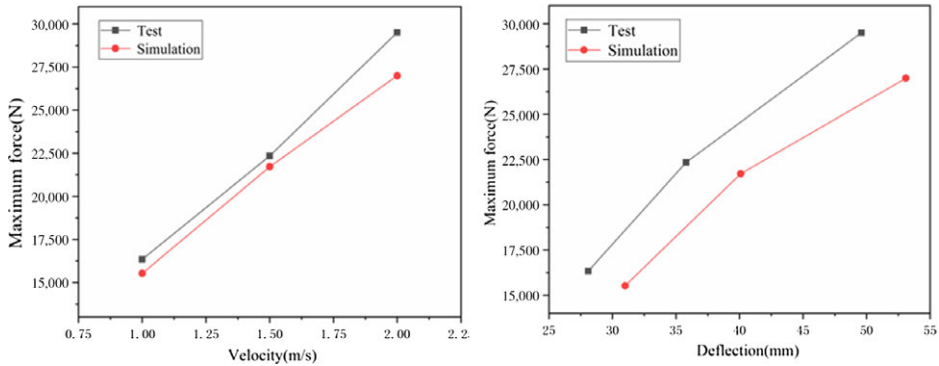
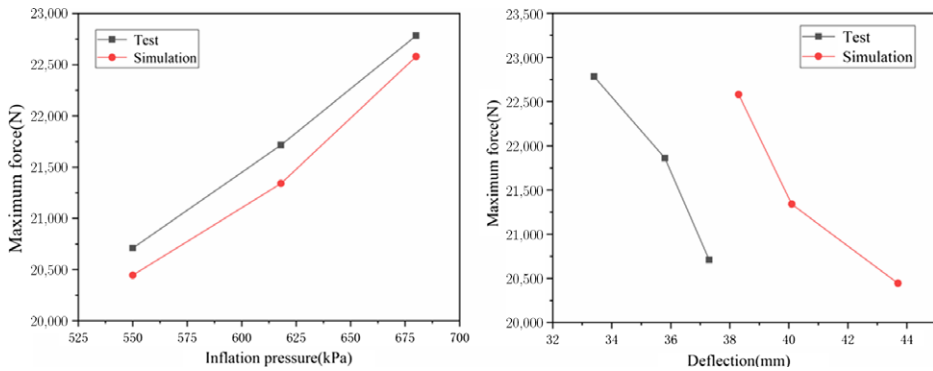Figure 13. Force versus velocity and force versus deflection in case B.

Figure 14. Force versus inflation pressure and force versus deflection in case C.

In case B, in terms of the influence of velocity, the load increases approximately linearly with speed (Fig. 12). At 2m/s, the average experimental load is 29,506N, compared with the numerical value of 26,995N, that is, 8.5% smaller (Fig. 13). In a real landing scenario, higher velocity will lead to non-linear changes in load.

Case C mainly studies the effect of inflation pressure on load (Fig. 14). Comparison between cases A, B and C indicates that the inflation pressure has less effect on the impact load than do the impact mass and velocity. It is worth noting that the maximum stress in belts changes from a von Mises stress of 560MPa at an internal pressure of 618kPa to a von Mises stress of 606MPa at 680kPa. This is because of the more effective contact between the rim and tyre when the internal pressure is increased.

It should be emphasised that the range of impact velocities was relatively moderate, but still sufficient to cause tyre failure in some over-load cases. In a real landing scenario, tyres fail at a much higher velocity because the landing gear includes a shock absorber, which was not considered in this work. An aircraft tyre is a rubber product, and rubber has an obvious strain rate effect. Because the range of impact velocities was moderate, possible strain rate effects on the material properties were neglected in this study. As shown in Fig. 13, when the velocity was increased from 1.5 to 2m/s, the deviation between the test and simulation became larger. When the impact velocity becomes large enough, the strain rate effect of the material can no

Table 8
Test conditions in case A

Test case A number	Release height (mm)	Impact weight (kg)	Inflation pressure (kPa)
1	113.9	246.8	618
2	114.2	295.7	618
3	113.5	357.2	618

Table 9
Results in case A

Test case A number	Test force (N)	Simulation (N)	Deviation (%)	Test tyre deflection (mm)	Simulation (mm)	Deviation (%)
1	22,341	21,716	2.8	35.8	40.1	12.0
2	24,083	22,523	6.5	40.6	43.5	7.1
3	26,392	25,571	3.1	42.5	48.1	13.1

Table 10
Test conditions in case B

Test case B number	Release height (mm)	Impact weight (kg)	Inflation pressure (kPa)
1	50.8	246.8	618
2	113.9	246.8	618
3	200.1	246.8	618

Table 11
Results in case B

Test case B number	Test force (N)	Simulation (N)	Deviation (%)	Test tyre deflection (mm)	Simulation (mm)	Deviation (%)
1	16,343	15,531	5.0	28.1	31.0	12.1
2	22,341	21,716	2.8	35.8	40.1	12.0
3	29,506	26,995	8.5	49.6	53.1	13.1

longer be ignored. In the future, it will be necessary to develop a tyre model considering the strain rate effect of materials (rubber and belts), which would be suitable for different vertical velocity and load conditions.

The main results of the various impact scenarios are listed in Tables 8–13.

Table 12
Test conditions in case C

Test case C number	Release height (mm)	Impact weight (kg)	Inflation pressure (kPa)
1	113.0	246.8	550
2	113.5	246.8	618
3	115.7	246.8	680

Table 13
Results in case C

Test case C number	Test force (N)	Simulation (N)	Deviation (%)	Test tyre deflection (mm)	Simulation (mm)	Deviation (%)
1	20,710	20,445	1.3	37.3	43.7	17.1
2	21,860	21,340	2.4	35.8	40.1	12.0
3	22,783	22,580	1.0	33.4	38.3	14.6

7.0 CONCLUSIONS

This study investigated the impact response of aircraft tyres, including the rim in detail. The study used a special setup to enable the impact of a mass dropped onto the tyres. The displacements and loads in the impact scenario were monitored using a high-speed camera and force sensors. The experimental data were then compared with numerical simulations of the tests using the finite element method.

It can be concluded that the numerical model well captured the significant aspects of the impact events. This study could help tyre engineers improve aircraft tyre performance in the design phase. This may lead to a better overall response of aircraft tyres and landing gear shock absorbers, which could improve the safety of aircraft during landing. Very little experimental data is publicly available to verify aircraft tyre models. Therefore, the experimental data in this paper address this gap in the literature.

No attempt was made here to measure the material properties of actual tested tyres, opting to use instead material properties provided by the tyre manufacturer. However, the good agreement between the experiments and simulation indicates that this strategy was valid.

REFERENCES

1. KURUPPU, K.D.D. and HETTIARACHCHI, C.J. Case study on aircraft tyre wear in Y12 aircraft tyres. *Aeronaut. J.*, 2018, **122**, pp 1123–1144.
2. KILNER, J.R. Pneumatic tire model for aircraft simulation. *J. Aircr.*, 1982, **19**, pp 851–857.
3. ANSON, R., PENA, J. and POSTIC, R. Finite element analysis applied to radial aircraft tyre engineering. *Proc. Inst. Nech. Eng. G*, 1996, **210**, pp 109–116.
4. BEHROOZI, M., OLATUNBOSUN, O.A. and DING, W. Finite element analysis of aircraft tyre – effect of model complexity on tyre performance characteristics. *Mater. Des.*, 2012, **35**, pp 810–819.
5. REID, J.D., BOESCH, D., BIELENBER, R.W. Detailed tyre modelling for crash applications. *Int J. Crashworthiness*, 2007, **12**, pp 521–529.

6. Guo, H., Bastien, C., Blundell, M. and Wood, G. Development of a detailed aircraft tyre finite element model for safety assessment, *Mater. Des.*, 2014, **53**, pp 902–909.
7. Baranowski, P., Malachowski, J., Janiszewski, J. and Wekezer, J., Detailed tyre FE modeling with multistage validation for dynamic analysis, *Mater. Des.*, 2016, **35**, 810–819.
8. Yao, S., Yue, Z., Geng, X. and Wang P. Finite element analysis of aircraft tire for safety assessment with CV and CPM methods, *Multidisc. Model. Mater. Struct.*, 2017, **13**, pp 501–508.
9. Essienubong, I.A., Ikechukwu, O.and Paul, S. Finite element analysis of aircraft tire behaviour under overloaded aircraft landing phase. *Aeron Aero Open Access J.*, 2018, **2**, pp 32–37.
10. Zhang, X., Xu, F., Ren, X., Gao, X. and Cao, R. Consideration on aircraft tire spray when running on wet runways, *Chin. J. Aeronaut.*, 2020, **33**, pp 520–528.
11. Xia, Y., Yong, X. and Li, W. Study on the compressible hyperelastic constitutive model of tire rubber compounds under moderate finite deformation, *Rubber Chem. Technol.*, 2004, **77**, pp 230–241.
12. Tanner, J.A., Daugherty, R.H. and Smith, H.C. *Mechanical Properties of Radial-ply Aircraft Tires.* SAE 2005-01-3438, USA: SAE International, 2005.
13. Ojala, J.K. *Using ABAQUS in tire development process.* In: ABAQUS users' conference 2005, Pawtucket, USA; October 14, 2004.
14. Smith, L.P. *The Language of Rubber: An Introduction to the Specification and Testing of Elastomers*, Butterworth-Heinemann Ltd., 1993, London, p 257.
15. Chagno, G., Marckmann, G. and Verron, E. A comparison of the Hart-Smith model with Arruda-Boyce and gent formulations for rubber elasticity, *Rubber Chem. Technol.*, 2004, **77**, pp 724–735.
16. Ali, A., Hosseini, M. and Sahari, B.B. A review of constitutive models for rubber-like materials. *Am. J. Eng. Appl. Sci.*, 2010, **3**, pp 232–239.
17. Mooney, M. A theory of large elastic deformations. *J. Appl. Phys.*, 1940, **11**, pp 582–592.
18. Rivlin, R.S. Large elastic deformations of isotropic materials: Fundamental concepts. *Philos. Trans. R. Soc. A*, 1948, **240**, pp 459–490.
19. Hall, W., Mottram, J.T. and Jones, R.P. Finite element simulation of a rolling automotive tyre to understand its transient macroscopic behavior. *Proc. Inst. Mech. Eng. D*, 2004, **218**, pp 1393–1408.
20. Naser, B., Kaliske, M. and Andre, M. Durability simulations of elastomeric structures. In Austrell, P.E. and Kari, L. (Eds), *Constitutive Models for Rubber IV*, AA Balkema Publishers, Rotterdam, Netherlands, 2005, p 45–50.
21. Shiraishi, M., Iwasaki, N., Saruwatari, T. and Hayashi, K. Developing FE-tyre model library for durability and crash simulations. 7th European LS-DYNA Users' Conference, Salzburg, May, 2009.
22. Danielson, K.T., Noor, A.K. and Green, J.S. Computational strategies for tyre modelling and analysis, *Comput. Struct.*, 1996, **61**, pp 673–693.
23. Wong, J.Y. *Theory of Ground Vehicles*, 2nd edition, John Wiley & Sons, Inc. New York, 2008.
24. Clark, S.K. *Mechanics of Pneumatic Tires*, U.S. Department of Transportation, Washington, DC, 1981.
25. Federal Aviation Administration, "Aircraft tires", TSO-C62, Washington, DC, 2006.